Volume 66, Issue 3, 2022
Journal of Scientific Research
of
The Banaras Hindu University

Study of electronic structure, electrical characteristics and transport properties of heteroatoms (N, O & S) based Anthracene molecular Nanowires-A DFT Study

Jayalakshmi Palaniappan[1], Jothi Balakrishnan[2], Selvaraju Karuppannan[3*], David Stephen Arputharaj[4], and C Pitchumani Violet Mary[5]

[1]Kandasami Kandar's College, Velur, Namakkal, manijaya2003@gmail.com
[2]Kandasami Kandar's College, Velur, Namakkal, jothiphysics@09@gmail.com
[3*]Kandasami Kandar's College, Velur, Namakkal, physicsselvaraj@gmail.com
[4]PSG College of Arts and Science, Coimbatore, stevepearlin@gmail.com
[5]Sri Shakthi Institute of Engineering and Technology, mviolet88@gmail.com

Abstract: **For designing the electronic devices using molecular wires, it is important to understand the electronic properties at the molecular level. In this paper, the simulation methodology for analyzing the electrical conductivity of anthracene conjugated molecule sandwich between Au atoms via linker Sulfur atom, is proposed. This theoretical analysis is carried out for different applied electric field ranges from 0 to 0.26 VÅ^{-1} to metal electrode Au atom using density functional theory (DFT). The effect of external applied electric field towards the structural variation of metal attached anthracene molecule [WH] is well explored and compared the results with that of hetero atoms [N, S, and O] substituted heterocyclic systems [HAA, HTA and HOA]. Further, the ability of electron flow through these systems were explored from the analysis frontier molecular orbitals and density of states (DOS). The bonding nature of the studied molecules were well described from the QTAIM analysis and finally the reactive sites for electrophilic and nucleophilic attack was identified from the simulation of molecular electrostatic potential surface. Non-covalent interaction (NCI-RDG) analysis is addressed to characterize the interactions in heteroatom substituted anthracene based molecular nanowires. In our overall study, the outcomes are exposing that the significates feature and importance of electrical conductivity nature and transport characteristic of hetero-atoms (N, S, O) substituted anthracene based molecular nanowires.**

Index Terms: **Anthracene molecular nanowire, hetero- atoms, DFT study, QTAIM and NCI-RDG analysis.**

I. INTRODUCTION

The reduction of size of the conventional electronic devices is getting really an interesting effort and more puzzling as they prevent the hardware from functioning adequately in size less than 10nm. Practical impediments on semiconductor manufacture and preparing methods additionally make it more troublesome and costly to manufacture electronic circuits at these profound nano-scale levels. The size reduction is really accomplished by invoking the molecular wires in the circuit (Vilan A., et al., 2017, Yutaka W.,et al., 2008, Erik G., et al., 2019).The conjugated molecules are entertained in the molecular wires, from which the charge transport over the long distance is achieved.(Rohrer H.,et al., 2008) A few sorts of molecules have been recommended as molecular wires up until this point, they all have similar key necessities (Selvaraju K., Kumaradhas P.2015, Selvaraju K.,et al.,2013, Srinivasan P., et al (2009). Planning and incorporating of upgraded molecular wires might be worked with by hypothetical strategies with more solid prescient capacities. Quantum chemical computations utilizing DFT approach was carried out to meet out the experimental results. In the current investigation, we report the theoretical and computational accomplishments of molecular orbital examination on anthracene molecule with the heteroatoms

DOI: 10.37398/JSR.2022.660331 257-272

substituted at 1 and 3 position of six membered ring; Nitrogen, Sulfur and Oxygen mentioned hereafter as HAA, HTA and HOA. The data from the above investigation is compared for the molecule [WH] having no heteroatoms. These heterocyclic compounds have been appended with gold (Au) atoms at the two terminals through Sulfur linker between the molecule and metal terminals (Fig 1).

II. COMPUTATIONAL DETAILS

Density functional theory (DFT) calculations were carried out for the optimization of Au and heteroatoms (N, S &O) substituted haxaanthracene molecules by varying applied electric fields from 0 VÅ^{-1} to 0.26 VÅ^{-1}. The significant variations in topological properties of the electron density which includes electron density, Laplacian of electron density and total energy density at the (3,-1) bond critical point in the bonding regions, and electrical conductivity [from the band gap analysis] of heteroatom containing anthracene molecule were calculated under the applied electric filed between 0 VÅ^{-1} to 0.26 VÅ^{-1}. The variations of the above-mentioned properties for the applied electric field beyond 0.26 VÅ^{-1}, were very feeble, hence, the molecule has been applied to the external field up to 0.26 VÅ^{-1}. All the calculations were performed at Becke's three parameters exchange function and Lee, Yang and Parr gradient-corrected correlation function B3LYP/6-31G(d,p) (Becke A.D. (1993) was used for C, H, N, O, S atoms and basis set of LANL2DZ (Los Alamos National Laboratory of Double Zeta) (McC B.J. (1986)) used for Au (gold) atoms.The gold atoms [Au] at the either side of the molecule was played a role of electrode via Sulphur linker which facilitates the charge transport through the anthracene molecule. Thus, there would be no variation in the electrical conductivity when the single Au atom was replaced by the cluster. Frequency calculations have been analyzed to characterize the minima on the potential energy surface and which has shown no imaginary frequencies for all three molecules. Various quantum chemical properties are also calculated by using the following theoretical background (Jaiswal V., et al., 2014).

$$\chi = -\mu \quad = -\left(\frac{\partial E}{\partial N}\right)_{v(r)}$$

In general, chemical hardness (η) (Kaya S., Kaya C. 2015) is a second derivative of energy of an atomic and molecular system with respect to the number of electrons (N). Hardness is used as a measure of resistance to changes in the electron distribution of a system

$$\eta \quad = \frac{1}{2}\left(\frac{\partial^2 E}{\partial N^2}\right)_{v(r)}$$

According to the following operational and approximate definitions of Parr and Pearson (Parr R.G,. Pearson R.G . 2002), the global hardness (η) and softness (S) are calculated

$$S = \frac{1}{(IE - EA)} \qquad \eta = \frac{(IE - EA)}{2}$$

where IE and EA are first vertical ionization energy and electron affinity of the molecule respectively. The global electrophilicity index (ω) (Parr R.G.,et al.,1999) is calculated by using chemical potential and hardness as

$$\omega = \frac{\mu^2}{2\eta}$$

Further, the ionization energy (IE) and electron affinity (EA) were calculated based on the Koopmans' theorem (Tsuneda T., et al.,2010), by using the following relation,

$-\varepsilon_{HOMO} = IE \qquad -\varepsilon_{LUMO} = EA$

So, the approximate definition of hardness and chemical potential can be written as follows:

$$\eta = \frac{E_{LUMO} - E_{HOMO}}{2} \qquad \mu = \frac{E_{LUMO} + E_{HOMO}}{2}$$

In addition to NCI analysis (Laplaza R.,et al.,2021) , a detailed Bader's topological analysis Kumar(P.S.V., et al.,2016) has been carried out from QTAIM perspective to address these weak interactions at molecular level. The essential wave functions for the NCI-RDG and QTAIM calculations have been generated at the B3LYP/6-31G(d,p)/LANL2DZ level. Natural bond orbital analysis (NBO) (Glendening E.D.,et al.,2019) has been carried out at the same level to analyses the stabilizing interactions of these HA molecules. All these calculations were performed using Gaussian09 package (Gaussian.com,).

III RESULTS AND DISCUSSION

Scheme 1 illustrates the 1,4,5,8,9,10-hexaanthracene (HA) along with different heteroatoms N (-aza), S (-thia), O (-oxa) considered for the present study. Our focus is to understand the behaviour of heteroatoms with anthracene-based frameworks for the better transport properties. In this study, our aim is to cognize the role of heteroatoms on molecular nanowire behavior of anthracene with two gold (Au) atoms at the end of the terminals. In which, Au (gold) acts as metal

anodes for applying for the various electric fields at the two terminals. Then, it would be fascinating to see how heteroatoms alter the structural and electrical characteristics of these molecules. Among the three heteroatoms, effect of heteroatoms has been studied and evaluated for their electrical characteristics for the molecular nanowire applications where only applied for an electric field from 0 $VÅ^{-1}$ to 0.26 $VÅ^{-1}$. These three molecules namely HAA, HTA and HOA with nitrogen (N), Sulfur (S) and Oxygen (O) atoms substitutions respectively. This nomenclature is followed throughout this paper.

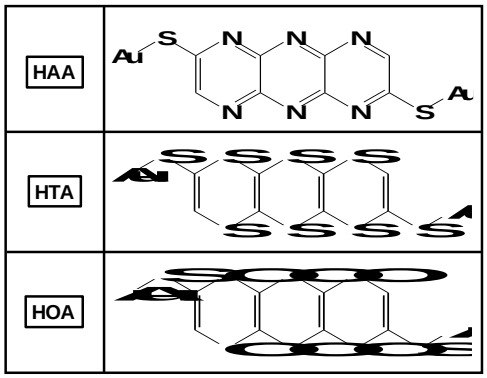

Scheme 1**.** Structure of Gold attached with various hetero atoms of anthracene molecules.

A. Geometry Optimization

The important structural parameters of the optimized (at gas phase) geometries (HAA, HTA & HOA) were shown for the zero field to maximum applied field of 0.26 $VÅ^{-1}$ in Fig 1. The selected bond parameters of (particular & average) bond lengths (Å) and bond angles (˚) were listed in Table 1. From the DFT calculation, it is observed that most of the C-C bond lengths and C-C-C bond angles in WH (without heteroatom) system are similar. The average value of C-C bond length and C-C-C bond angle for WH system are 1.410 Å and 120.4˚ respectively. In WH molecule, the L_{end} Au-S bond elongates from 2.329 Å to 2.368 Å when the field increased from 0 $VÅ^{-1}$ to 0.26 $VÅ^{-1}$ and this could be the maximum varying only the bond lengths and there is no much deviation in terminal bond angles towards the applied EFs. Similar trend was noticed for the right edge $_{WH}$C-S-Au bond angle, which is increased by 3.2˚ (from 103.9˚ to 107.1˚), whereas the left edge $_{WH}$C-S-Au gets increased by 1.70˚ towards the applied EF. For the three selected molecular nanowires, Au atom has attached at the end of terminal position of Right (R_{end}) and terminal position of Left (L_{end}) through sulfur atom (S). Upon substitution of heteroatoms in anthracene molecules, the variation in the bond lengths of C-S and S-Au by varying the applied electric field ranges from 0 $VÅ^{-1}$ to 0.26 $VÅ^{-1}$were shown in Fig1 and Fig1A.

In this optimization, upon introducing of heteroatom of nitrogen (N) into molecule HAA, the molecular gains aromaticity when compared to WH molecule. The average bond length of $_{HAA}$C-C is found to be slightly higher (1.447 Å to 1.449 Å) for increasing the applied filed field from 0 $VÅ^{-1}$ to 0.26 $VÅ^{-1}$ when compared with that of WH molecule (1.410Å). In other hand, both the terminal positions (L_{end} and R_{end}) are found to have the slightly higher $_{HAA}$C-S (1.781 Å) bond length at zero electric field. For the maximum applied field of 0.26 $VÅ^{-1}$, both the L_{end} and R_{end} bond lengths ($_{HAA}$C-S) are slightly altered and reduced to 1.776 Å and 1.761 Å respectively. Notably, the variation of two terminal position of (R_{end} and L_{end}) bond lengths of S-Au are found to shorten compared with WH molecule (zero field) which is clearly given in Table 1. The R_{end} of $_{HAA}$C-S-Au decreased by 13.6˚ from the respective angle in WH molecule under 0.26 $VÅ^{-1}$, whereas the L_{end} of $_{HAA}$C-S-Au was increased by 3˚. On the application of external EF, there is no significant bond length variation. The bond length of left side $_{HAA}$C-S bond gets contracted by 0.032 Which is the maximum variation calculated when the EF varies from 0.21 $VÅ^{-1}$ to 0.26 $VÅ^{-1}$. Opposite trend is found for R_{end} of $_{HAA}$C-S bond, whereas the bond length is increased from 1.760 Å to 1.776 Å when the EF varies from 0.21 $VÅ^{-1}$ to 0.26 $VÅ^{-1}$. Up to 0.21 $VÅ^{-1}$, there is no significant changes in the terminal bond angles. When EF changes from 0.21 $VÅ^{-1}$ to 0.26 $VÅ^{-1}$, R_{end} of $_{HAA}$C-S-Au decreased by 13.6˚ and L_{end} of $_{HAA}$C-S-Au get increased by 6.4 deg. Similar trend happens for terminal C-C-S; R_{end} of $_{HAA}$C-C-S decreased by 6.2˚. However, when introducing heteroatoms of nitrogen atom introduced in (HAA), the molecule achieved aromaticity remain as such same when compared to WH molecule but only the changes for the slightly altering the two terminals bond distance C-S an S-Au.

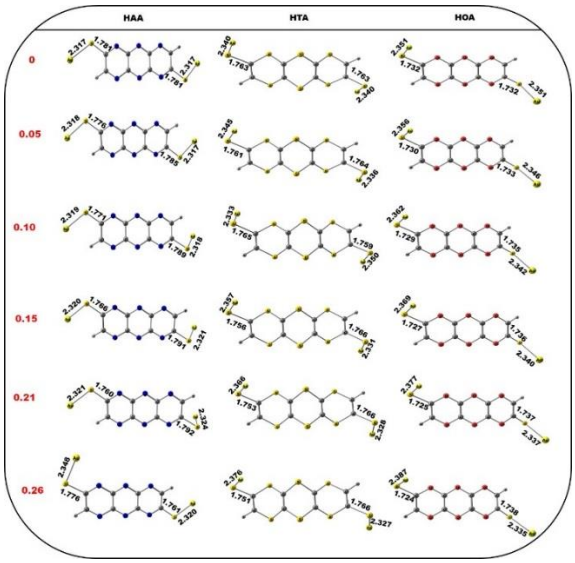

Fig 1. The terminal bond length variation of optimized geometries of (a) HAA, (b) HTA, and (c) HOA under applied electric field from 0 VÅ^{-1} to 0.26 VÅ^{-1}. For HTA, the bond length of right-side Au-S bond gets elongated by 0.043 Å, which is the maximum variation calculated when the EF varies from 0 VÅ^{-1} to 0.26 VÅ^{-1}. The increment pattern gets break at EF 0.15 VÅ^{-1}, where the length decreased slightly by 1.5 Å, then the increment pattern persists up to EF 0.26 VÅ^{-1}. Similar scenario was observed in bond angle variation and maximum variation (2.47˚) is found for the angle $_{HTA}$C-S-Au at L_{end}, the angle is increased from 101.6˚ to 103.6˚ on the application of EF increased from 0 VÅ^{-1} to 0.26 VÅ^{-1}. Like the bond length variation, at 0.15 VÅ^{-1}, the increasing pattern get braked by slight decrement by 1.5˚. Also, the maximum bond twist of about 10˚ is observed, on the application of external EF 0.26 VÅ^{-1}, for the bond S-C bond at the L_{end}. As expected, the rings in HTA system is not coplanar and sulfur (S) atom attributes the distorted geometry. The S atoms at both R_{end}/L_{end} rings and mid ring are at 0.540 Å and 0.668 Å distances from the central plane framed from carbon atoms of the individual rings.

In HOA, for the external applied EF from 0 VÅ^{-1} to 0.26 VÅ^{-1}, the maximum variation (0.036 Å) in the bond length is noticed for right edge Au-S bond varies from 2.351 Å to 2.381 Å. The opposite trend was calculated for left edge Au-S bond, where the bond length values were decreased from 2.351 Å to 2.335 Å. Like HAA, and HTA, the L_{end}C-S-Au hits for the maximum bond angle variation (1.3˚) towards the applied EF, and the angle was increased from 102.8˚ to 104.1˚. Similar trend was noticed for R_{end}C-S-Au and angle is varied by 0.81˚ on the application of EF from 0 VÅ^{-1} to 0.26 VÅ^{-1}. From the above analysis, it is concluded that the applied external EF influences more on the bond angles, in more specific, the external applied EF attributes the significant variation in the terminal region of HAA system when compared with other conjugated systems. Overall, the calculated geometric parameters imply that planarity can be tuned by varying the heteroatoms and different electrical field ranges from 0 VÅ^{-1} to 0.26 VÅ^{-1}. These are very important for their molecular nanowire properties.

B. Frontier Molecular Orbital (FMO) and Energetic Analysis

In material science, frontier molecular orbitals (FMOs) have been used to become important information on the charge transport properties of molecules (Chamani Z., et al 2014) which is mainly associated with highest occupied molecular orbitals (HOMOs) and lowest unoccupied molecular orbitals (LUMOs)(Eliziane S.,et al., 2019, Caruso F.,et al.,2014).Therefore, in order to understand and examine the nature of the FMOs (HOMO-2, HOMO-1, HOMO, LUMO, LUMO+1, LUMO+2) has been depicted in Fig. 2. HOMO orbitals are mainly involved in the unit of with and without heteroatoms substituted anthracene rings. In other hand, LUMOs are predominantly associated and stabilized with the two terminal positions of S-Au atoms. The heteroatoms substituted anthracene unit is highly stabilized on the HOMO part. This can be clearly indicating that the charge transfer takes place from heteroatom substituted units to terminal positions of S-Au atoms

Table 1. Selected geometrical parameters of the conjugated systems. Bond lengths in (Å) and Bond angles in (˚)

Molecules	HAA		HTA		HOA		WH	
	0	0.26	0	0.26	0	0.26	0	0.26
Selected Bond Length (Å) of Two Terminals (L_{end} and R_{end})								
$(C\text{-}C)_{avg}$	1.447	1.449	1.346	1.348	1.340	1.342	1.410	1.411
$(C\text{-}S)_{right}$	1.781	1.776	1.763	1.751	1.732	1.724	1.778	1.768
$(C\text{-}S)_{left}$	1.781	1.761	1.763	1.766	1.732	1.738	1.778	1.759
$(C\text{-}N)_{avg}$	1.336	1.337	-	-	-	-	-	-

$(C\text{-}S)_{avg}$	-	-	1.783	1.782	-	-	-	-
$(C\text{-}O)_{avg}$	-	-	-	-	1.378	1.378	-	-
$(Au\text{-}S)_{right}$	2.317	2.348	2.340	2.376	2.351	2.387	2.329	2.321
$(Au\text{-}S)_{left}$	2.317	2.320	2.340	2.327	2.351	2.335	2.329	2.368
Selected Bond Angles (°) of Two Terminals (L_{end} and R_{end})								
$(C\text{-}S\text{-}Au)_{right}$	106.2	94.2	101.6	101.4	102.9	103.6	103.9	107.1
$(C\text{-}S\text{-}Au)_{left}$	106.2	108.6	101.6	103.6	102.9	104.1	103.9	105.6
$(C\text{-}C\text{-}S)_{right}$	124.4	118.4	120.4	120.1	122.0	121.8	120.8	123.5
$(C\text{-}C\text{-}S)_{left}$	124.4	125.0	120.4	120.8	122.0	122.8	120.8	120.8

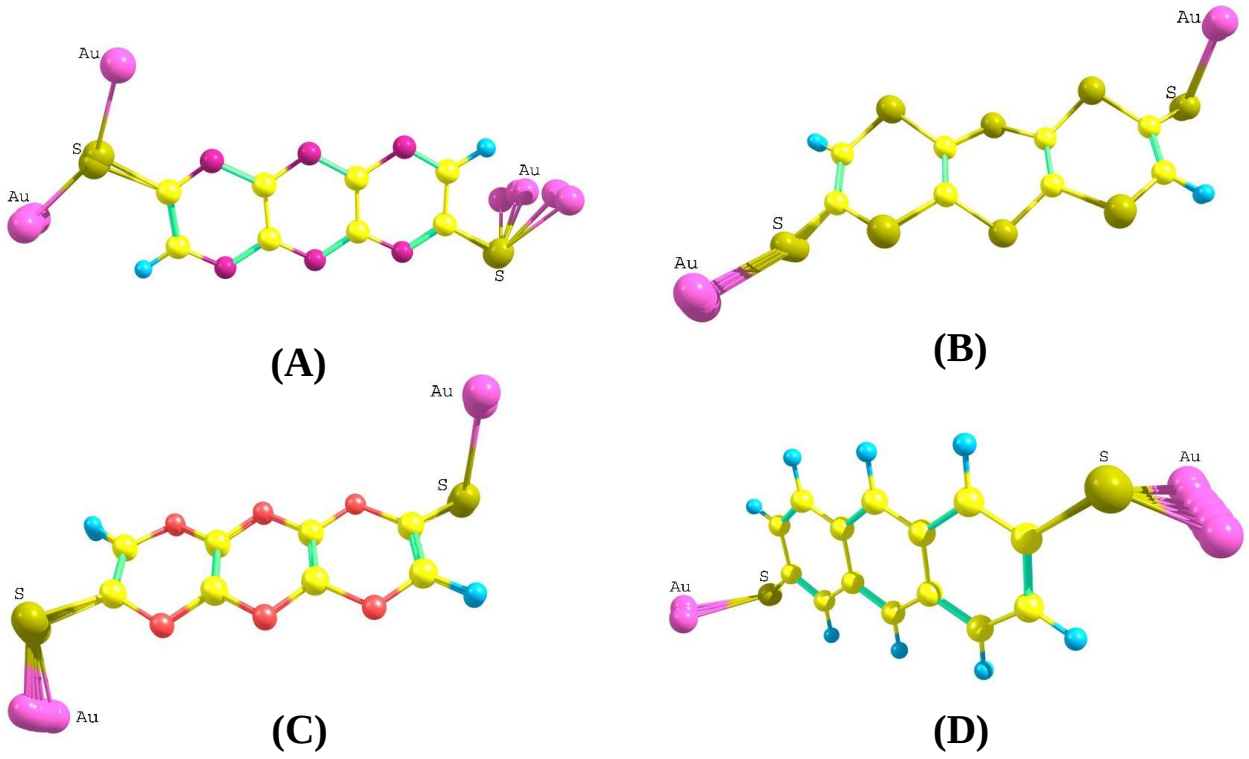

Fig 1A. The superimpose of optimized geometries of (a) HAA, (b) HTA, (c) HOA, and (d) WH under applied electric field from 0 $VÅ^{-1}$ to 0.26 $VÅ^{-1}$

.

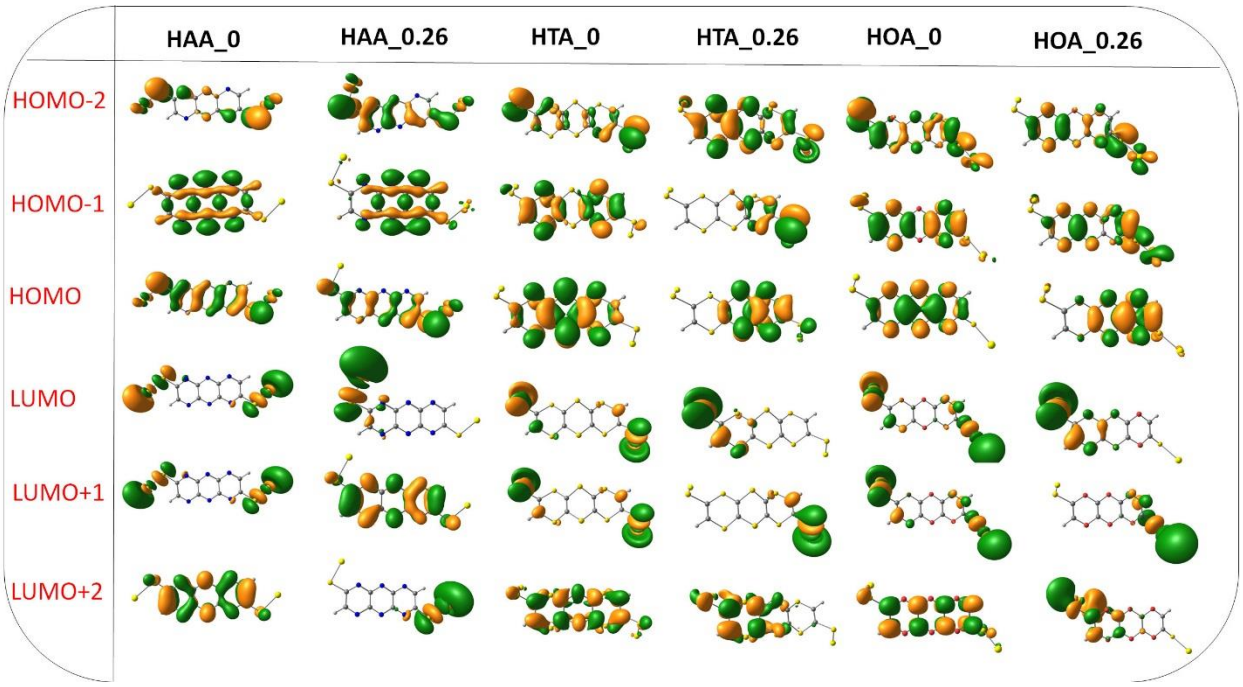

Fig 2. The FMO's (HOMO-2 to LUMO+2) of the molecules.

The FMO energy levels and their corresponding HOMO-2 to LUMO+2 values are shown in Fig 2. Particularly, HOMO-LUMO gaps are given for the applied field of zero to maximum EF for all molecules in Table 2. Among the three molecules, HAA was found to have the highest H-L gap of 2.34 eV (at zero electric filed) whereas three molecules have been shown on the value of 1.77 eV for (HTA) and 1.59 eV (for HOA) respectively. The HOMO-LUMO gaps are gradually reduced for all the molecules not only for the applied electric field of 0–0.26 VÅ^{-1} but also changing the heteroatoms (N, S, & O atoms). This can be implying that the applied filed localizes the HOMO-LUMO orbitals of the molecules. The smaller the energy band gap facilitates the electron transfer from HOMO to LUMO energy levels. Also, the chemical reactivity was well understood from HOMO-LUMO energy levels (E_g) whereas HOA molecules is found to have higher reactive molecule (lowest E_g of 0.79 eV) at the maximum applied electric field when compared with HTA (0.18 eV) and HAA (1.51 eV). This can be clearly indicating that the HOA molecule can has higher conductivity for increases the EF from zero to maximum.

In Fig 2, among the all molecule shows that at 0.26 VÅ^{-1} all the systems improve the conductivity nature which is attributed from minimum band gap values, the values are listed in the Table 1. From this observation, it is clear that these heteroatoms-based molecules are expected to perform well in molecular nanowires. Particularly, Energy gap results has been in the following order of HOA < HTA < HAA. Moreover, LUMO can be highly stabilization for the energy gaps by introducing of heteroatoms of N, S & O in anthracene molecules. This can be clearly noticed that the heteroatoms will help to alter the LUMO level which is mainly play a crucial role on the suitable substitution of the molecules.

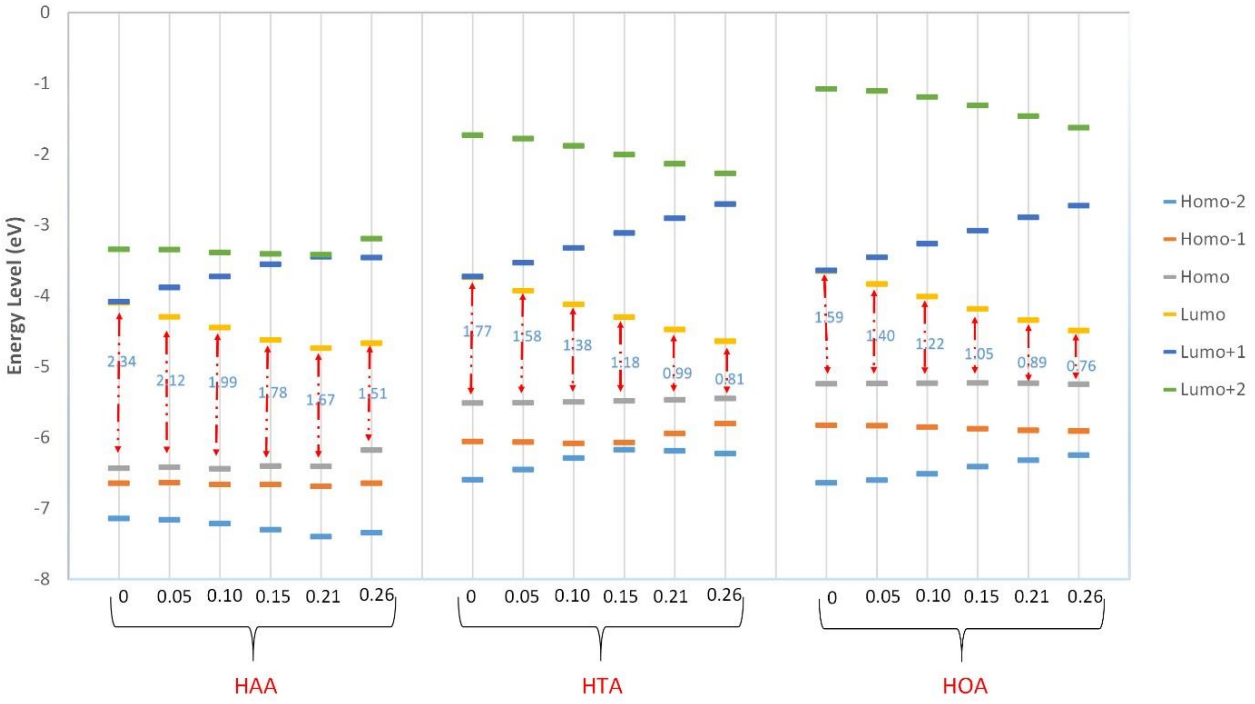

Fig 3. Energy Band gap variation of the hetero atom substituted systems under various

From the Table 3, it is noticed that among the systems, HTA and HOA having Sulfur and oxygen atoms achieved narrow energy band gap of about ~0.8eV, reflects the prominent electrical conductivity nature. This attribute the influence of hetero atom types in the charge transport over the molecular nano-wires. To gain more insights from into the HOMO-LUMO orbitals [FMOs], FMO orbital compositions and their respective energetics have been shown in Fig 3. The hetero atom substituted systems, [HAA, HTA, and HOA] and WH molecules were segmented into four units includes electrode atom, Au [metal], right ring [RR], left ring [LR] and mid ring [bridge] to get more insights of FMO's and their energetics. Figure 6 clearly reveals that the LUMO of all the conjugated systems were highly stabilized [~95%] by electrode, Au atoms, especially when the molecule is under the influence of 0.26 VÅ^{-1} applied electric field. In overall molecules, heteroatom (with and without) substituted anthracene units contributes towards the highly delocalized in HOMOs whereas LUMO is also stabilized by Au-S units. Especially, anthracene ring of HOA molecule (bridge ring) is providing for the larger contribution takes place from HOMO to LUMO at the applied electric field of both (0 and 0.26 VÅ^{-1}). Overall, the lower H-L gap can assist for the charge transfer and electron conduction from HOMO to LUMO orbitals. Also, LUMO orbitals are highly stabilized by Au-S units which can attributes the maximum contributions of 80-90%. Hence, Au-S attached anthracene (N, O & S substituted) molecules can act as effective molecular nanowire applications. By the substitution of different heteroatoms [N, S and O] in the anthracene molecule, the electrical conductivity was highly influenced at 0.26 VÅ^{-1}. It is noticed that among the systems, HTA and HOA having Sulphur and oxygen atoms achieved a narrow energy band gap of about ~0.8eV [Kindly refer Table 2 in the manuscript], reflects the prominent electrical conductivity nature. This attributes the influence of hetero atom types in the charge transport over the molecular nano-wires. This was well visualized in figure 3.

Table 2. Energy Band gap (E_g) values of the with and without heteroatoms substituted anthracene systems for different applied electric field

Molecules	Band Gap for Applied Electric Field (in VÅ^{-1})					
	0	0.05	0.10	0.15	0.21	0.26
WH	2.03	1.94	1.76	1.58	1.41	1.27

HAA	2.34	2.12	1.99	1.78	1.67	1.51
HTA	1.77	1.58	1.38	1.18	1.00	0.81
HOA	1.59	1.40	1.22	1.05	0.90	0.76

C. Optoelectronic properties

Examining the electronic properties of heteroatom substituted anthracene-based molecules gives information about the energetics, charge transport and conductivity nature of the systems. Based on HOMO and LUMO energy values, the electronic properties such as ionization potential [IP], electron affinity[EA], Chemical potential [μ], Electronegativity [χ], Hardness [η], Softness [S] and Electrophilic index [ω] of the molecules under the minimum [0 VÅ^{-1}] and maximum [0.26 VÅ^{-1}] applied electric field were calculated and the values are listed in the Table 3.

Table 3. Electronic properties of the conjugated systems for the applied electric field 0 VÅ^{-1} and 0.26 VÅ^{-1}. (The values are in eV).

Molecules (EF in VÅ^{-1})		IP	EA	μ	χ	η	S	ω
WH	0	5.64	3.61	-4.62	4.62	1.02	0.49	10.52
	0.26	5.43	4.16	-4.79	4.79	0.63	0.79	18.11
HAA	0	6.44	4.10	-5.27	5.27	1.17	0.43	11.87
	0.26	6.18	4.67	-5.42	5.42	0.75	0.66	19.48
HTA	0	5.51	3.74	-4.62	4.63	0.89	0.56	12.07
	0.26	5.45	4.64	-5.05	5.05	0.40	1.23	31.44
HOA	0	5.24	3.65	-4.45	4.45	0.79	0.63	12.44
	0.26	5.25	4.49	-4.87	4.87	0.38	1.31	31.17

From the Table 3, it is revealed that the IP value of HAA molecule is higher when compared with other molecules, which shows its increasing tendency to capture electrons. This was further supported from EA values which measure the strength of the acceptor, the corresponding EA value is 4.669eV [at 0.26 VÅ^{-1}] which is the maximum value found among the other molecules. The least EA value is found for WH system. It is also noted that the average chemical potential (μ) for HAA, HTA and HOA molecules at 0 V Å^{-1} and 0.26 VÅ^{-1} are calculated as -4.8 eV and -5.1 eV respectively, and these were the smallest values of μ, compared to WH system. This attributes that WH system has the tendency to escape the electron and system having hetero atoms to attract the electrons. This tendency of HAA, HTA and HOA molecules was established from maximum electronegativity values, 5.424, 5.047 and 4.870 eV at 0.26 VÅ^{-1}. From the values of electrophilic index (ω), the conjugated systems [HAA, HTA and HOA] involving hetero atoms [N, S and O] are having the good capability of accepting electrons when compared with the system [WH] having no heteroatoms. In particular, the electrophilic nature was strengthened significantly from ~12eV to ~31eV for HTA and HOA systems when the applied electric field is increased from 0 VÅ^{-1} to 0.26 VÅ^{-1} respectively. On the whole, HTA and HOA systems are the good donor of electrons and possess higher electrical conductivity. Nearby HOMO and LUMO orbitals may influenced the electrical conductivity of the heteroatom substituted systems. So, only the HOMO and LUMO level consideration may not give a proper description of frontier orbitals. Thus, the total density of states (TDOS) was calculated using GaussSum package(O'Boyle N.M., et al.,2008, Adak O., et al.,2015,Badorrek J.,Walter M.2021) , which gives the contributions of different molecular composition in the chemical bonding. Since the electrical conductivity is found to be increased at the electric field 0.26 VÅ^{-1}, the corresponding TDOS for all the systems were plotted and shown in the Fig 4 (a-d). Here, the broaden nature of DOS peaks attributes the hybridization of the molecule and electrode (Au) orbitals.

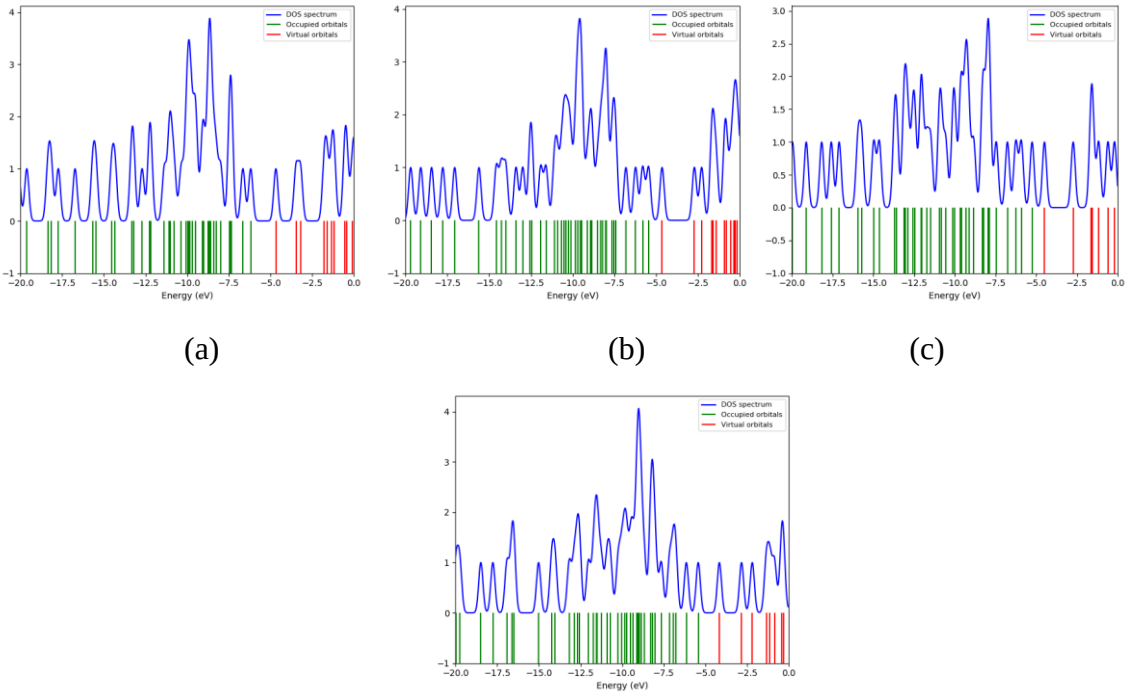

Fig 4 (a-d). The TDOS plot of (a) HAA, (b) HTA, (c) HOA and (d) WH systems

D. QTAIM analysis

The chemical bonding of all the systems were characterized from Bader's theory of Quantum theory of atoms in molecules (Esser S. (2019). This theory also predicts the energetic nature which relates to the bond density, Laplacian of electron density at the (3, -1) bond critical point. All possible (3, -1) critical point search was done for all homo and hetero atomic bonds.

There is no significant variation is observed in the calculated topological parameters when the electric field is increased from 0 $VÅ^{-1}$ to 0.26 $VÅ^{-1}$, and therefore the topological parameters predicted at 0.26 $VÅ^{-1}$ is considered for the discussion and the corresponding values are listed in the table 5. The pictorial representation of (3, -1) bond critical points of all the systems are shown in the Fig 5.

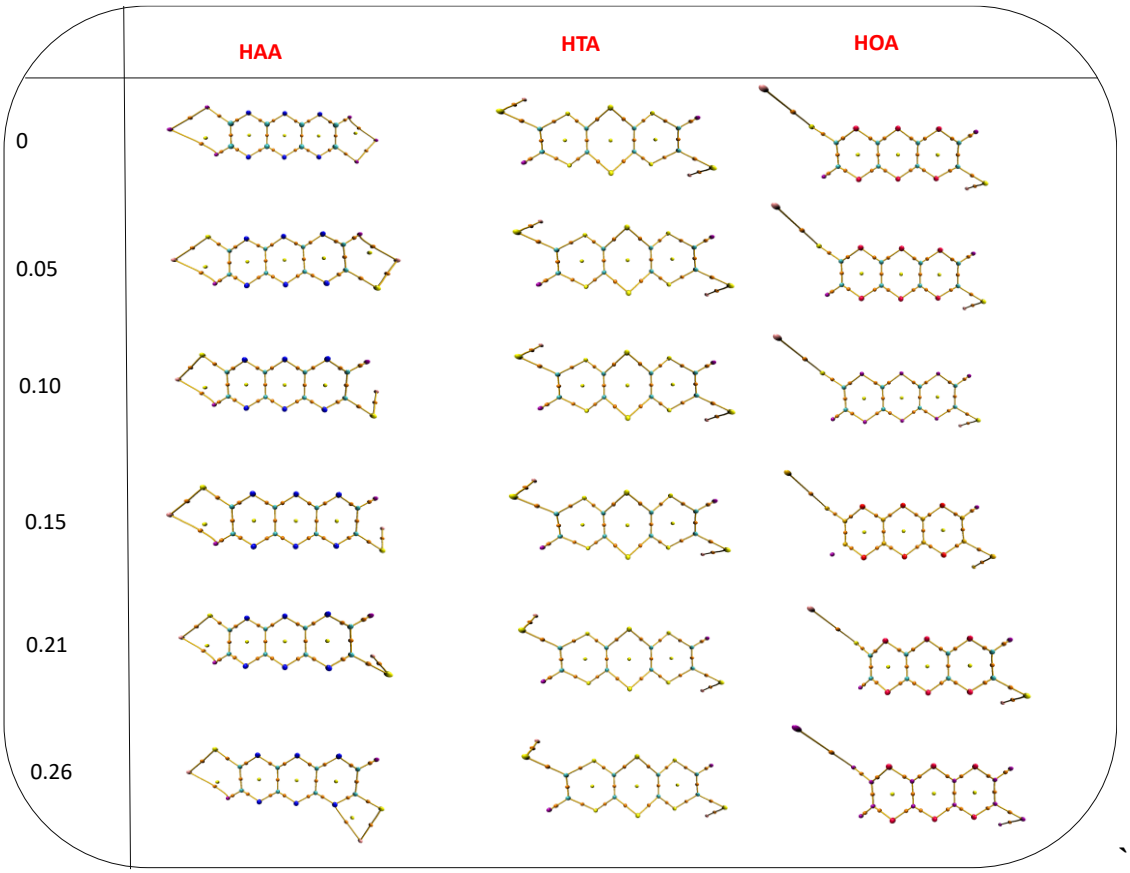

Fig 5. The molecular graph showing (3, -1) critical points of (a) HAA, (b) HTA and (c) HOA. Orange sphere represents the bcp.

From the Table 5, it is revealed that the lowest bond density is found for Au-S bond and the average value is 0.603 eÅ^{-3}. The Laplacian of electron density [$\nabla^2\rho_{bcp}(r)$], has been raised from second order partial derivative of electron density, which quantifies the curvature of the function in 3D. The negative value of Laplacian directs to the locally concentrated charges at the bcp and a positive value leads to the locally depleted. The covalent nature of C-S, C-N, C-O and C-C bonds was well confirmed from the negative Laplacian of electron density values and exhibiting an open-shell interaction. The closed-shell type Au-S interaction was evident from the positive values of Laplacian [3.50 eÅ^{-5}].

Table 4. The average topological parameters of molecules at (3, -1) bond critical points calculated for 0.26 VÅ^{-1} applied electric field.

Selected Bonds	HAA		HTA		HOA		WH	
	ρ_{bcp} (eÅ^{-3})	$\nabla^2\rho_{bcp}$ (eÅ^{-5})	ρ_{bcp} (eÅ^{-3})	$\nabla^2\rho_{bcp}$ (eÅ^{-5})	ρ_{bcp} (eÅ^{-3})	$\nabla^2\rho_{bcp}$ (eÅ^{-5})	ρ_{bcp} (eÅ^{-3})	$\nabla^2\rho_{bcp}$ (eÅ^{-5})
Au-S	0.610	3.63	0.603	3.44	0.591	3.49	0.608	3.45
$(S\text{-}C)_{terminal}$	1.338	-9.3	1.327	-8.83	1.398	-10.53	1.333	-8.81
$(C\text{-}N)_{HAA}$	2.34	-24.4	-	-	-	-	-	-
$(C\text{-}S)_{HTA}$	-	-	1.290	-8.15	-	-	-	-
$(C\text{-}O)_{HOA}$	-	-	-	-	1.899	-9.86	-	-
$(C\text{-}C)_{WH}$	-	-	-	-	-	-	2.059	-19.84

E. Natural Bond Orbital (NBO) Analysis

In order to get clearer insight into the effect of applied electric field on the inter- and intramolecular delocalization, from NBO(Salami N.,Shokri A., 2021, Weinhold F.,2012), second order perturbation theory analysis has been carried out for the optimized structures of HAA, HTA, HOA and WH molecules respectively and the obtained results were presented in table 6. Since the higher values of stabilization energy indicates the strongest stabilization, the interactions with stabilization energy greater than 6 kcal/mol has been considered for the analysis. From the obtained results it is inferred that the inclusion of electric-field induces the changes in the delocalization like BD-LP*, BD-BD*, and LP-BD* respectively. On comparing the orbital delocalization of HAA, HTA, HOA and WH molecules, the HAA and WH molecule was observed with highest stabilization energy for all type of delocalization and found to be in the range of 25 – 78kcal/mol given in Table 5. Whereas, for HTA and HOA molecules the stabilization energy for BD-LP* and BD-BD* delocalization was found to be in the range of 6 – 7 kcal/mol and for LP-BD* delocalization, it is observed that 10-35 kcal/mol.

Table 5. NBO analysis of the conjugated systems for the applied electric field 0 VÅ^{-1} and 0.26 VÅ^{-1}.

Molecule	**Donor NBO**	**Acceptor NBO**	**Stabilization Energy (kcal/mol)/ (EF in** VÅ^{-1})					
			0	**0.05**	**0.10**	**0.15**	**0.21**	**0.26**
HAA	BD (2) C1 - N6	LP*(1) C5	39.28	40.37	42.00	43.46	45.19	36.56
	BD (2) C2 - N3	BD*(2) C4 - N7	21.36	21.58	21.71	21.92	22.07	20.56
	BD (2) C4 - N7	LP*(1) C5	29.99	29.67	29.51	29.08	28.51	31.24
	BD (2) C4 - N7	LP (1) C8	57.52	57.41	56.55	56.00	54.76	56.54
	BD (2) C9 - N10	LP*(1) C5	57.52	57.60	58.26	58.43	59.10	57.59
	BD (2) C9 - N10	LP (1) C8	29.98	30.23	30.16	30.11	29.85	27.28
	BD (2) N11 - C12	LP (1) C8	39.28	38.30	37.31	36.88	37.08	45.24
	BD (2) C13 - N14	BD*(2) C9 - N10	21.36	21.16	21.48	21.50	21.94	22.87
	LP (1) C8	BD*(2) C4 - N7	65.18	64.05	62.81	61.25	59.16	69.22
	LP (1) C8	BD*(2) C9 - N10	73.64	74.07	74.04	73.97	73.52	74.66
	LP (1) C8	BD*(2) N11 - C12	56.49	57.61	59.24	61.41	64.83	54.44
	LP (2) S18	BD*(2) C1 - N6	21.92	23.23	25.23	26.56	27.99	23.85
HTA	BD (1) C3 - H17	BD*(1) C4 - S 5	6.92	6.99	6.78	6.88	6.83	6.76
	BD (1) C13 - H18	BD*(1) S11 - C14	6.92	6.85	7.05	6.93	6.94	6.95
	BD (1) S15 -Au19	BD*(2) C3 - C4	6.03	6.31	5.54	6.07	6.07	6.05
	BD (1) S16 -Au20	BD*(2) C13 - C14	6.03	5.77	6.61	6.11	6.21	6.33
	LP (2) S 2	BD*(2) C1 - C6	15.10	15.64	14.12	15.90	16.05	16.06
	LP (2) S 2	BD*(2) C3 - C4	17.18	17.73	16.28	20.98	22.09	22.87
	LP (2) S 5	BD*(2) C1 - C6	14.39	15.03	13.30	15.12	15.29	15.35
	LP (2) S 5	BD*(2) C3 - C4	11.46	11.90	10.71	13.19	13.54	13.64
	LP (2) S 7	BD*(2) C1 - C6	11.75	11.65	12.06	12.54	13.02	13.63
	LP (2) S 7	BD*(2) C8 - C9	11.94	12.19	11.50	11.69	11.71	11.79
	LP (2) S10	BD*(2) C1 - C6	11.94	11.71	12.47	12.42	12.68	13.00
	LP (2) S10	BD*(2) C8 - C9	11.75	11.89	11.61	11.48	11.54	11.67

	LP (2) S11	BD*(2) C8 - C9	14.39	13.81	15.68	14.03	13.99	14.11
	LP (2) S11	BD*(2) C13 - C14	11.46	11.08	12.29	9.94	9.56	12.97
	LP (2) S12	BD*(2) C8 - C9	15.10	14.60	16.18	14.46	14.26	14.16
	LP (2) S12	BD*(2) C13 - C14	17.18	16.69	18.28	14.19	13.47	12.97
HOA	BD (2) C1 - C2	BD*(1) S12 -Au14	6.95	7.28	7.61	7.90	8.13	8.27
	BD (1) C2 - H9	BD*(1) C1 - O19	6.97	6.90	6.84	6.77	6.69	6.61
	BD (2) C7 - C8	BD*(1) S11 -Au13	6.94	6.61	6.28	5.97	5.69	5.42
	BD (1) C8 - H10	BD*(1) C7 - O16	6.95	6.99	6.98	6.96	6.93	6.91
	BD (1) S11 -Au13	BD*(2) C7 - C8	6.98	6.99	7.03	7.10	7.23	7.38
	BD (1) S12 -Au14	. BD*(2) C1 - C2	6.97	6.94	6.89	6.85	6.83	6.82
	LP (2) O15	BD*(2) C5 - C6	26.67	26.97	27.02	27.06	27.15	27.38
	LP (2) O15	BD*(2) C7 - C8	29.95	28.94	27.72	26.52	25.40	24.45
	LP (2) O16	BD*(2) C5 - C6	28.64	28.90	28.85	28.87	29.05	29.47
	LP (2) O16	BD*(2) C7 - C8	22.81	22.40	21.45	20.54	19.67	18.97
	LP (2) O17	BD*(2) C3 - C4	27.48	28.05	28.67	29.31	29.98	30.63
	LP (2) O17	BD*(2) C5 - C6	25.96	25.42	24.78	24.13	23.65	23.40
	LP (2) O18	BD*(2) C3 - C4	25.98	26.53	27.12	27.67	28.19	28.64
	LP (2) O18	BD*(2) C5 - C6	27.48	26.96	26.42	25.86	25.51	25.42
	LP (2) O19	BD*(2) C1 - C2	23.10	23.30	23.69	23.86	23.89	23.80
	LP (2) O19	BD*(2) C3 - C4	28.79	28.48	28.33	28.19	28.15	28.25
	LP (2) O20	BD*(2) C1 - C2	30.03	30.98	31.94	32.79	33.49	33.92
	LP (2) O20	BD*(2) C3 - C4	26.76	26.42	26.20	26.01	25.92	25.96
WH	BD (2) C1 - C25	LP*(1) C4	34.60	35.49	36.80	38.45	40.51	42.92
	BD (2) C1 - C25	BD*(2) C2 - C23	14.78	14.74	14.58	14.44	14.24	13.98
	BD (2) C2 - C23	BD*(2) C1 - C25	15.18	15.24	15.30	15.36	15.45	15.58
	BD (2) C2 - C23	BD*(2) C3 - C21	16.87	17.07	17.15	17.27	17.32	17.29
	BD (2) C3 - C21	LP*(1) C4	42.48	42.51	42.41	42.34	42.20	41.97
	BD (2) C3 - C21	LP (1) C5	49.80	50.01	49.76	49.54	48.99	48.17
	BD (2) C3 - C21	BD*(2) C2 - C23	17.50	17.32	17.24	17.15	17.13	17.20
	BD (2) C6 - C19	LP*(1) C4	49.80	49.44	49.07	48.31	47.34	46.18
	BD (2) C6 - C19	LP (1) C5	42.48	42.42	42.23	41.96	41.58	41.09
	BD (2) C6 - C19	BD*(2) C8 - C17	17.50	17.68	17.83	18.01	18.14	18.25
	BD (2) C7 - C15	LP (1) C5	34.60	33.88	33.51	33.38	33.57	34.11
	BD (2) C7 - C15	BD*(2) C8 - C17	14.78	14.78	14.82	14.76	14.68	14.59
	BD (2) C8 - C17	BD*(2) C6 - C19	16.87	16.66	16.50	16.26	16.05	15.86
	BD (2) C8 - C17	BD*(2) C7 - C15	15.18	15.12	15.02	14.90	14.73	14.54
	LP (1) C5	BD*(2) C3 - C21	65.50	65.00	64.31	63.61	62.83	62.02
	LP (1) C5	BD*(2) C6 - C19	57.53	57.23	56.84	56.16	55.32	54.33
	LP (1) C5	BD*(2) C7 - C15	63.46	65.76	68.70	71.52	74.46	77.27

F. Molecular electrostatic potential [MEP]

The calculation of molecular electrostatic potential has been carried out to understand the physiochemical properties (Fedorov D.G.,et al.,2019, Lu T.,Chen F.2012, Prakash Chandra R., et al.,2020). which includes the reactive sites for electrophilic and nucleophilic regions. The MEP plots were plotted for all the systems under the 0.26 VÅ^{-1} applied electric field. The relative polarity of these molecules was well distinguished from this calculation. The variably charged regions of these conjugated systems were visualized from MEP plots.

In general, the electrophilic regions were identified from the negative regions [red] of electrostatic potential surface, and the positive regions [blue] relates the nucleophilic reactivity. In Fig 6, the blue, white and red regions identify the different surfaces of electrostatic potential varying from -0.05 to +0.13 au; blue and yellow spheres represent minima and maxima ESP surface respectively. Irrespective of the conjugated systems, it was found that ESP surface minima is found near the electrode atom [Au] at the left side; whereas the surface maxima were found at the right-side Au atom.

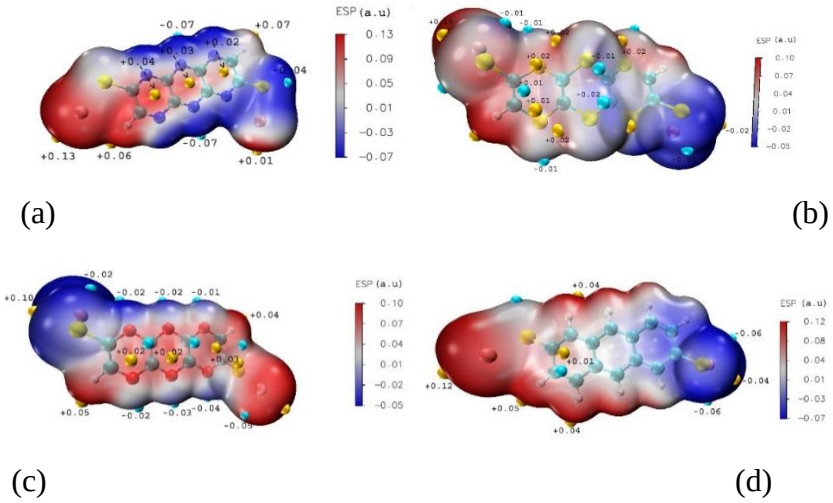

Fig 6. The ESP-mapped molecular surface of (a) HAA, (b) HTA, (c) HOA and (d) WH molecules. The Units in a.u. Local maxima and minima are represented by yellow and blue spheres.

Fig 7 (a-d) shows the surface areas of all the systems in different ESP ranges. From these figures it is clear that large portion of the surface covers the ESP values ranges from -20 to +20 kcal/mol. Also, the variance of ESP in both the positive and negative regions were calculated for all the systems. The corresponding values are 253.51/117.52 kcal/mol, 114.02/58.41 kcal/mol, 121.38/52.40 kcal/mol and 180.74/104.77 kcal/mol for HAA, HTA, HOA and WH respectively. These values reveal that ESP distribution fluctuates remarkably in HAA system, as their polarity index is 17.5 kcal/mol which is the maximum value; whereas the polarity index for HTA, HOA and WH were calculated as 11.16 kcal/mol, 13.09 kcal/mol and 15.82 kcal/mol respectively.

G. Non-covalent interactions (NCI) Analysis

NCI-RDG analysis is carried out on the optimized geometries of selected four molecules which is representing stabilizing attractive (blue), destabilizing repulsive (red) and weak van der waals interactions (green) isosurfaces respectively. The reduced density gradient [RDG] and its corresponding isosurface was obtained from Multiwfn software (Pettersen E., 2004). RDG is calculated to identify the NCI regions (Boto R.A.,2015). RDG isosurface can be used to analyze the strength of the interactions under the value of 0 and 0.26 VÅ^{-1} applied electric fields. The RDG scatter plot was shown in the Fig 8 which has based on the sign of (λ_2) ρ and their respective values in HAA, HTA and HOA at 0 VÅ^{-1} and 0.26 VÅ^{-1}. The HAA molecule found to show the values of (λ_2) -0.01 a.u (green – weak interactions) and 0.01 to below 0.03 a.u (red – repulsive) under 0 to maximum electric field of 0.26 VÅ^{-1} whereas the isosurface value of -0.02 au (blue color – large negative) is present strong attractive region. In HTA, repulsive and weak interactions regions were shown in the ranges between 0 to -0.01 (red) and 0 to 0.02 (red) under 0 to maximum electric fields. By the changing of electric field between zero and maximum (0.26 VÅ^{-1}) in HOA molecule, there is obtained only for the repulsive forces (large positive - red region) ranges between 0.02 to 0.03 a.u. In other hand, there is no attractive (blue) and weak interactions while introducing with (0.26 VÅ^{-}

[1]) and without (zero) electric fields in molecules HOA. The heteroatom atom of (oxygen) substituted HOA molecule found to have increases the red region (repulsive) which has been implied that the higher electrical conductivity than compared to other molecules.

CONCLUSION

The ability of electrically conductive nature of with and without hetero atoms [N, S, and O] anthracene molecules were examined by using DFT approaches under the influence of various applied electric field ranges from zero VÅ^{-1} to 0.26 VÅ^{-1}. Among the four systems, it is predicted that when the electric field is increased from 0 to 0.26eV, HAA system [nitrogen hetero atom substituted] shows some slight geometrical variations at the terminal region. From the FMO analysis, it is predicted that HTA and HOA systems having Sulfur and oxygen atoms attained narrow energy band gap of about ~0.8eV, reflects its prominent electrical conductivity nature. The calculation of ionization potential [IP] and electron affinity [EA] shows the substantial ability of electron capture of hetero atom substituted systems [HAA, HTA and HOA]. Also, the LUMO of all studied molecules was stabilized predominantly by the Au atoms under the maximum applied electric field [0.26 VÅ^{-1}]. The closed shell interaction of Au and S atoms of all the conjugated systems were well recognized from the positive values of Laplacian of electron density. Finally, the reactive sites of these systems were distinguished from MEP analysis and it is noticed that irrespective of all the studied molecules, the large portion of the surface covers the ESP values ranges from -20 to +20 kcal/mol and the ESP distribution fluctuates remarkably in HAA system. In NCI-RDG analysis, this can be highly witnessed for an enhancement of the electrical conductivity inside in the heteroatom substituted HOA molecule. In overall, our study not only emphasis the important of heteroatoms but also providing for the proper platform to developing a heteroatom substituted anthracene based molecular nanowires.

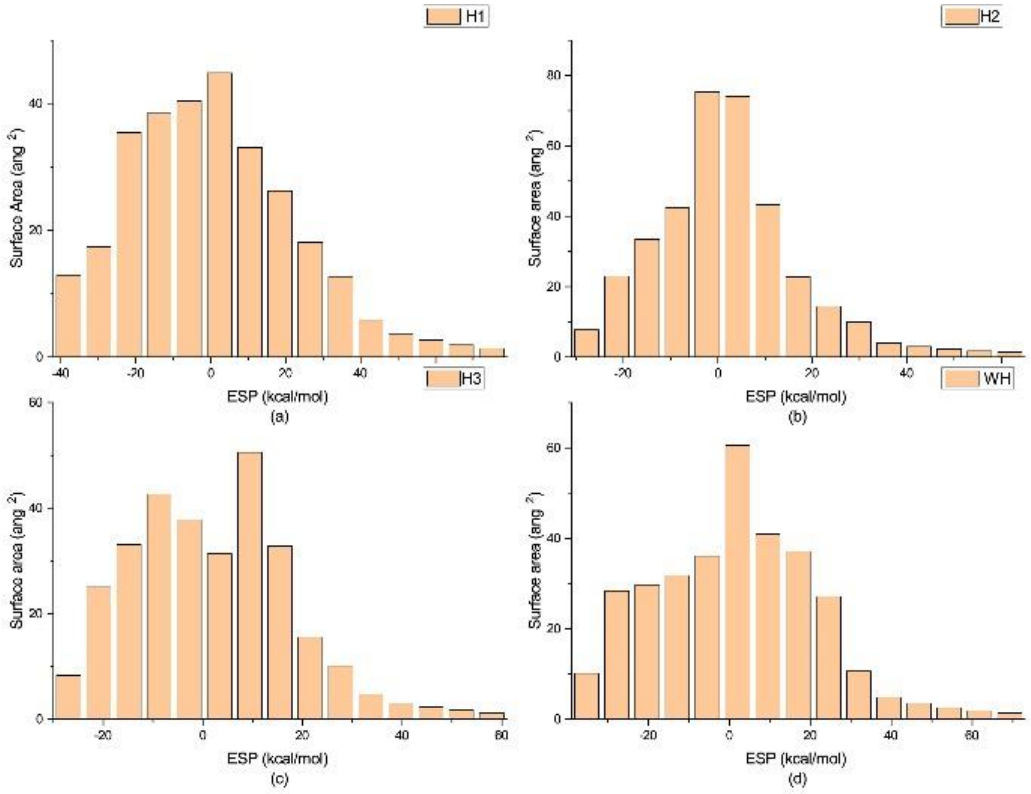

Fig 7. Surface area of (a) HAA, (b) HTA, (c) HOA and (d) WH systems in each ESP range.

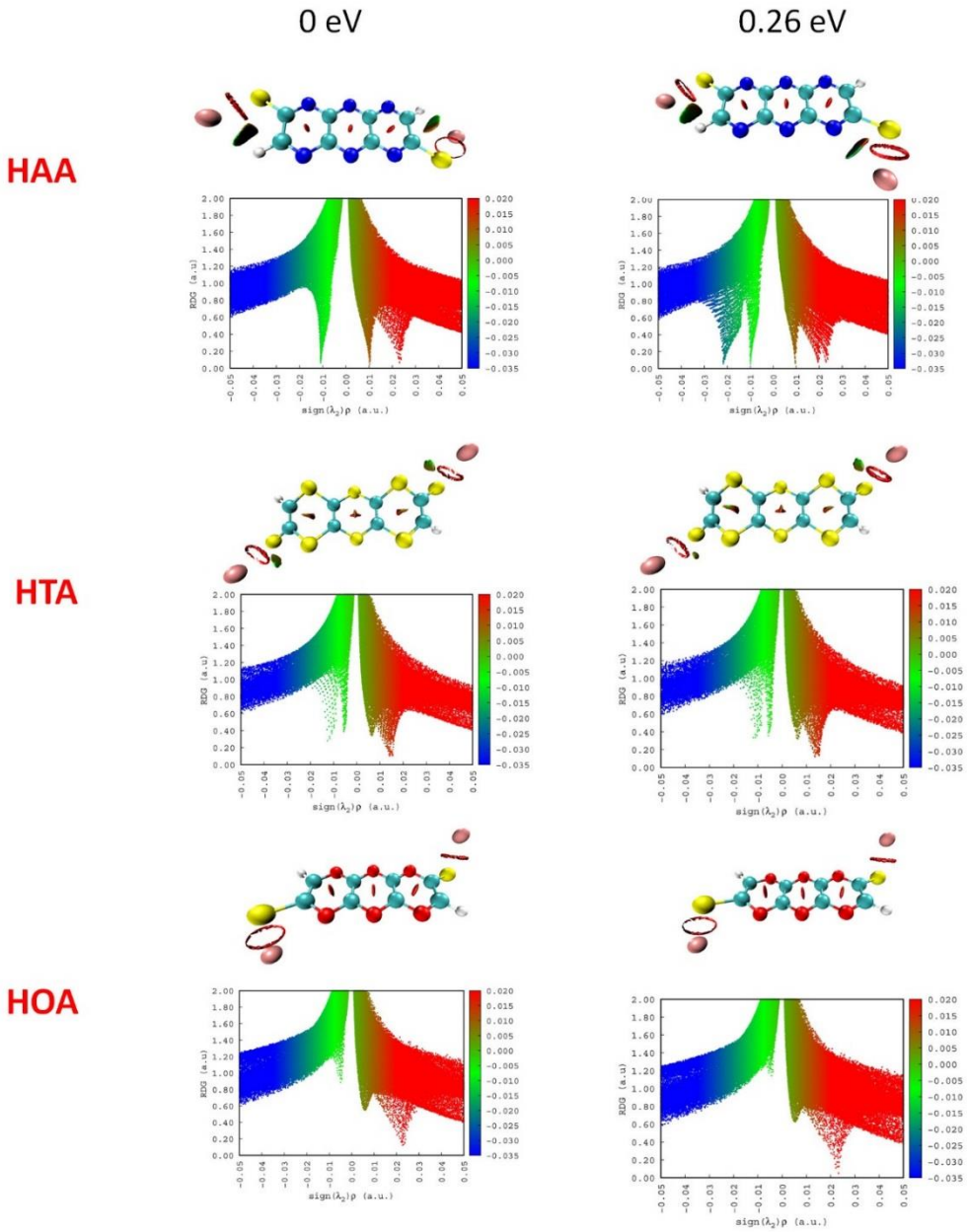

Fig 8. RDG scatter plot of heteroatom substituted molecules.

REFERENCES

Vilan A., Aswal D., Cahen D. (2017) Large-Area, Ensemble Molecular Electronics: Motivation and Challenges, Chem. Rev. 117, 4248–4286.

Yutaka W., Ryoma H., Toyohiro C., Shinichi M., Tomonobu N., Stefan E., Dimas G., de O., Helmut D., and Kenji, K. (2008) Self-Assembled Molecular Nanowires of 6,13-Bis(methylthio)pentacene: Growth, Electrical Properties, and Applications, Nano Letters.8 (10), 3273-7.

Erik G., Liqiang M., and Peidong Y. (2019) Introduction:1D Nanomaterials/Nanowires, Chemical Reviews. 119 (15),8955–8957

Rohrer H., Gerber C., Weibel E., Becker A,. Faisal F., Zhao Z., Lin C., Lee K., Rayner D., Corkum P.B., Villeneuve

D.M., Bandrauk A., Dwyer J.R.,Jordan R.E.,Miller R.J.D., Stapelfeldt H., Seideman T., Delone N.B., Krainov V.P., Spanner M., Smirnova O.,Ivanov M., Brabec T., Lein M., Marangos J., Knight P., Yurchenko S., Patchkovskii S., Litvinyuk I., Yudin G., Bordas C., Paulig F., Helm H., Huestis D., Eppink A., Parker D., Minemoto S., Sakai H. (2008) Electrical Resistance of Long, Science 320 ,1482–1486.

Selvaraju K., Kumaradhas P.(2015)Charge Density Analysis and Transport Properties of TTF Based Molecular Nanowires: A DFT Approach, J. Nanosci. 1–12.

Selvaraju K., Jothi M., Kumaradhas P. (2013) A charge density analysis on quarter thiophene molecular nanowire under applied electric field: A theoretical study, J. Comput. Theor. Nanosci. 10 ,357–367.

Srinivasan P., Stephen A.D., Kumaradhas P. (2009)Effect of gold atom contacts in the conjugated system of one-dimensional octane dithiolate based molecular wire: A theoretical charge density study, J. Mol. Struct. THEOCHEM . 910 ,112–121.

Becke A.D. (1993) Density-functional thermochemistry. III. The role of exact exchange, J. Chem. Phys. 98, 5648–5652. McC B.J. (1986) Gaussian basis sets for molecular calculations, J. Mol. Struct. *THEOCHEM*. 136, 201.

Jaiswal V., Rastogi R.B, Maurya J.L., Singh P., Tewari A.K. (2014) Quantum chemical calculation studies for interactions of antiwear lubricant additives with metal surfaces, RSC Adv. 13438–13445.

Kaya S., Kaya C. (2015) A new equation for calculation of chemical hardness of groups and molecules.113 ,1311–1319.

Parr R.G,. Pearson R.G . (2002) Absolute hardness:companion parameter to absolute electronegativity, J. Am. Chem. Soc. 105, 7512–7516.

Parr R.G., Szentpály L. V., Liu S. (1999) Electrophilicity Index, J. Am. Chem. Soc. 121, 1922–1924.

Tsuneda T., Song J.W., Suzuki S., Hirao K. (2010) On Koopmans' theorem in density functional theory, J. Chem. Phys.

Laplaza R ., Peccati F., Boto R. A., Quan C., Carbone A., Piquemal, J.P., MadayY., Contreras-García J. (2021) NCIPLOT and the analysis of noncovalent interactions using the reduced density gradient, Wiley Interdiscip. Rev. Comput. Mol. Sci.

Kumar P.S.V., Raghavendra V., Subramanian V. (2016) Bader's Theory of Atoms in Molecules (AIM) and its Applications to Chemical Bonding, J. Chem. Sci. 128, 1527–1536.

Glendening E.D., Landis C.R.,Weinhold F. (2019) NBO 7.0: New vistas in localized and delocalized chemical bonding theory, J. Comput. Chem. 40,2234–2241.

Gaussian 09 Citation | Gaussian.com, (n.d.).

Chamani Z., Bayat Z., Mahdizadeh S.J. (2014) Theoretical study of the electronic conduction through organic nanowires, Journal of Structural Chemistry. 55 (3) 530- 538.

Eliziane S., SantosVitória., ReisLuciana Guimarães Clebio S., NascimentoJr. (2019).Molecular wires formed from native and *push-pull* derivatives polypyrroles and β-cyclodextrins: A HOMO-LUMO gap theoretical investigation, Chemical Physics Letters. (730), 141-146.

Caruso F., Atalla V., Ren X, Rubio A., Scheffler M,. Rinke P. (2014). First-Principles Description of Charge Transfer in Donor-Acceptor Compounds from Self-Consistent Many-Body Perturbation Theory, Phys. Rev. B - Condens. Matter Phys. 90

O'Boyle N.M.,Tenderholt A.L.,Langner K.M. (2008). Cclib: A library for package-independent computational chemistry algorithms, J. Comput. Chem.

Adak O ., Korytár R., Joe A.Y., Evers F and Venkataraman L . (2015), Impact of Electrode Density of States on Transport through Pyridine-Linked Single Molecule Junctions Nano Lett. 6, 3716–3722.

Badorrek J.,Walter M:(2021) Computational study on noncovalent interactions between (n, n) single-walled carbon nanotubes and simple lignin model-compounds. Journal of Computational Chemistry.

Esser S. (2019) QTAIM and the Interactive Conception of Chemical Bonding, Philos. Sci. 86, 1307–1317.

Salami N.,Shokri A (2021) Electronic structure of solids and molecules, Interface Science and Technology 32, 325-373.

Weinhold F. (2012). Natural bond orbital analysis: A critical overview of relationships to alternative bonding perspectives. Journal of Computational Chemistry, *33*(30), 2363–2379.

Fedorov D.G., Brekhov A., Mironov V., Alexeev Y. (2019) Molecular Electrostatic Potential and Electron Density of Large Systems in Solution Computed with the Fragment Molecular Orbital Method, J. Phys. Chem. A. 123, 6281–6290.

Lu T.,Chen F.(2012)Multiwfn:A multifunctional wavefunction analyzer, J. Comput. Chem. 33,580–592.

Prakash Chandra R., Frederick L., and Marcel L.V. (2020). Practical High-Quality Electrostatic Potential Surfaces for Drug Discovery Using a Graph-Convolutional Deep Neural Network, Journal of Medicinal Chemistry, 63 (16),8778–8790.

Pettersen E., Goddard T., Huang C., Couch G., Greenblatt D., Meng E., and Ferrin T. (2004), UCSF Chimera - A Visualization System for Exploratory Research and Analysis,Journal of Computational Chemistry, 25 pp. 1605–1612.

Boto R.A., Contreras-García J.,Tierny J., Piquemal J.P. (2015) Interpretation of the reduced density gradient 114, 1406–1414.

***.